Journal of Solid Mechanics Vol. 12, No. 4 (2020) pp. 862-882
DOI: 10.22034/jsm.2019.1876588.1481

Analysis of Coupled Nonlinear Radial-Axial Vibration of Single-Walled Carbon Nanotubes Using Numerical Methods

A. Fatahi-Vajari [1, *], Z. Azimzadeh [2]

[1] *Department of Mechanical Engineering, Shahryar Branch, Islamic Azad University, Shahryar, Iran*
[2] *Young Researchers and Elite Club, Yadegar-e-Imam Khomeini (RAH) Shahre Rey Branch, Islamic Azad University, Tehran, Iran*

Received 26 July 2020; accepted 28 September 2020

ABSTRACT

This paper investigates the nonlinear-coupled radial-axial vibration of single-walled carbon nanotubes (SWCNTs) based on numerical methods. Two coupled partial differential equations that govern the nonlinear-coupled radial-axial vibration for such nanotube are derived using nonlocal doublet mechanics (DM) theory. To obtain the nonlinear natural frequencies in coupled radial-axial vibration mode, these equations are solved using Homotopic perturbation method (HPM). It is found that the coupled radial-axial vibrational frequencies are complicated due to coupling between two vibration modes. The influences of some commonly used boundary conditions, changes in vibration modes and variations of the nanotubes geometrical parameters on the nonlinear-coupled radial-axial vibration characteristics of SWCNTs are discussed. It was shown that boundary conditions and maximum vibration velocity play significant roles in the nonlinear-coupled radial-axial vibration response of SWCNTs. It was shown that unlike the linear one, the nonlinear natural frequencies are dependent to maximum vibration velocity. Increasing the maximum vibration velocity increases the natural frequency of vibration compared to the prediction of the linear model. However, with increase in tube length, the effect of the maximum vibration velocity on the natural frequencies decreases. It was also shown that the amount and variation of nonlinear natural frequencies are more apparent in higher vibration modes and two clamped boundary conditions. To show the accuracy and capability of this method, the results obtained herein are compared with the fourth order Runge-Kuta numerical results and also with the other available results and good agreement is observed. It is notable that the results generated herein are new and can be served as a benchmark for future works.

Keywords: Nonlinear coupled radial-axial vibration; Homotopic perturbation method; Nonlocal theory; Natural frequency; Single-walled carbon nanotubes.

1 INTRODUCTION

IT is well known that the mechanical behavior of heterogeneous solids is divided in two general viewpoints

[*] Corresponding author. Tel.: +98 21 65253181.
E-mail address: alirezafatahi@shriau.ac.ir (A. Fatahi-Vajari).

depending on the material phases are distributed continuous or discrete. Under continuous distribution, theories are based on continuum mechanics and do not contain scaling effects and this is normally regarded as a limitation to predicting micromechanical material behavior [1, 2]. Owing to nanoscale dimensions of carbon nanotubes (CNTs), it is difficult to set up controlled experiments to measure the properties of an individual CNT [3–5]. Also, molecular dynamics and atomistic methods [6–8] are costly and time-consuming to implement particularly for large-scale systems. In order to overcome this limitation, various elegant modifications to continuum mechanics have been proposed to incorporate scale and microstructural features into the theory. All of these theories are known as higher order gradient continuum theories. One of the most popular theories in micromechanics is doublet mechanics (DM) theory. DM was first developed by Granik and Ferrari [9] and it assumes that the stress tensor at a point is a function of strains at all points in the continuum. Carbon nanotubes (CNTs) invented by Iijima [10], have many unique properties. Their electro-mechanical property has explained in [11]. With rapid development in nanotechnology, nanotubes have great potential for wide applications as components in nano-electronic-mechanical systems (NEMS). Such nanostructures have received growing interest recently. Very often, these components are subjected to external loadings during work operation and then, understanding their dynamic behavior such as resonant properties is of much concern. As a result, Nano technological research on free vibration properties of nanotubes under certain support conditions is important because such components can be used as design components in Nano sensors and Nano actuators. At nanoscale, the mechanical characteristics of nanostructures are often significantly different from their behavior at macroscopic scale due to the inherent size effects. Size effects exist not only for mechanical properties but also for electronic, optical and some other properties. Owing to nanoscale dimensions of CNTs, it is difficult to set up controlled experiments to measure the properties of an individual CNT [12, 13]. In addition, atomistic methods [7, 8] are costly and time consuming to implement particularly for large-scale systems. The SWCNTs may be subjected to some heavy and complex dynamic loadings caused by different sources. By producing different states of stress, these loads might result in excess vibrations and may lead to failure. The vibrations of SWCNTs extremely affect the normal operation of the whole system and can lead to catastrophic failures in some cases [14- 16]. Due to the extensive applications and efficacy of CNTs, the precise prediction of the dynamic behavior of such systems is essential in their safety operation. Then, models should contain various factors that could represent the real dynamic behaviors of the system. Two important forms of vibrations that have been identified for SWCNTs are radial and axial vibrations. For example, for the flexible CNT with long span, high flexibility or being subjected to external excitations, the axial vibrations are important. Furthermore, if the CNT is assumed to be stretchable the radial deformations should be taken into account. So the study of the coupling between the vibrations of flexible SWCNT systems is of great importance. Furthermore form the literature, it is concluded that some other reasons can lead to the coupled radial-axial motion of the rotor such as crack and unbalancement [16]. Therefore, it can be concluded that axial and radial vibrations of the CNT systems are both significant, and sometimes it is important to considering the effect of coupling between radial and axial behavior of a SWCNT, especially for inspecting the CNTs instability conditions. It can be seen from the previous works on the vibration of SWCNTs that most of existing SWCNTs systems have concentrated on the flexural [17- 21], torsional [22- 25], radial [26, 27] or longitudinal [28- 31] vibrations behavior of the shafts, solely and the coupling effect between the others vibrational modes were ignored. The coupled vibration of SWCNTs is an interesting subject because of the complexity of the equations and the analytical solutions are difficult to obtain. Among them is radial-axial coupling in the vibrational behavior of the SWCNT system, which is originated from the large deformation of the beam. The radial-axial coupling vibration of the SWCNTs can lead to severe vibration, and this energy boosts the amplitude of the vibration and may leads to the early fatigue of tools and the reduction of bit life. If not taken into consideration, the effect of coupled vibration can not only reduce the calculation accuracy, but also lose some important characteristics of the CNTs. Therefore, it is important to establish an accurate model for dynamic characteristics of the coupled vibrations of CNTs. For the case of coupled radial-axial vibrations of the SWCNT, some nonlinearity can affect the total response of the system. It should be noted that in the linear analysis, axial and radial vibrations are decoupled and can be studied separately.

However, most of the investigations conducted on the radial and axial vibration of CNTs have been restricted to the linear theory. The HPM as a powerful analytical approach was first introduced by He [32, 33] for solving various linear and nonlinear initial and boundary value problems. The HPM in applied mathematics is widely studied now by most mathematicians and engineers. In this method, the solution is considered as the sum of an infinite series which converges rapidly to the exact solution. Usually, one or two iterations lead to high accuracy of the solution. The series used is a series of functions rather than terms as is in Taylor series. The method has recently been applied to a wide class of differential and integral equations, stochastic and deterministic problems, linear and non-linear equations. The advantages of this method to other methods is more simplicity, give better results and with time saving because in this method convergence is especially rapid in the nonlinear and nonhomogeneous equations. The

HPM was also studied by many mathematicians and engineers to investigate nonlinear equations arising in science and engineering. This simple method has been applied to solve linear and nonlinear equations in different fields of mechanics like heat transfer, fluid mechanics and so on [34- 36]. As known by authors, the combination of the geometric nonlinearity effects with the coupling of the radial-axial vibrations on the dynamic behavior of the SWCNTs is not investigated yet and the present work attempts to consider such analysis. Considering the complexity of the practical dynamics of the SWCNT systems, the main purpose of this study is investigating and modeling a mechanism for the coupled nonlinear radial-axial vibration of the SWCNTs. The governing differential equations for this case are obtained using nonlocal theory consist of two coupled partial differential equations with radial and axial displacements as the variables. These two coupled nonlinear equations are solved using HPM to obtain the natural frequencies which incorporate explicitly vibration velocity. This will reveal which key factors affect the coupled nonlinear radial-axial vibration and how they function, which can be a basis for the quantitative analysis of the coupling vibration of the SWCNTs. The fundamental frequencies of SWCNT in coupled nonlinear radial-axial vibration are validated with available results reported in literature. Then, HPM is applied to solve the nonlinear governing equations to obtain the nonlinear natural frequency equations for nonlinear-coupled radial-axial vibration of SWCNTs. Another aim of this investigation is to show the effectiveness of HPM and the capability of this simple method and also handling the nonlinear coupled axial-radial vibration for obtaining the nonlinear natural frequency. It is shown that the first approximate solution of New HPM admits a remarkable accuracy in comparison with the results obtained from the numerical method for the amplitude-frequency curves.

This manuscript is the extension of our previous papers [37] studied linear coupled axial-radial vibration of SWCNTs using DM. In [37], the linear coupled axial-radial vibration has been studied and the solutions are exact and analytical while in the present paper, nonlinear-coupled axial-radial vibration of SWCNTs via numerical methods (Galerkin and Homotopic Perturbation methods) studied. In this case, there is no exact solution for the natural frequency. To the best knowledge of the Authors, it is the first time that nonlocal DM theory has been used to analyze the nonlinear-coupled axial-radial vibration of SWCNTs. It should also be noted that in the previous work, only frequency domain is obtained but in this paper both time, domain and frequency domain is investigated. On the other hands, unlike [38], the frequency relations are given with analytical formulas. The structure of the paper is as follows. In Sect.2, a brief review to doublet mechanics is given. In sect.3, the nonlinear equation of motion for coupled radial-axial vibration of SWCNTs is derived using shell theory. In Sect.4, the equation of motion for SWCNTs in axial-radial vibration is solved using HPM and the natural frequencies are obtained. In Sect.5, the obtained nonlinear natural frequencies are compared with numerical results to illustrate the ability and accuracy of the proposed method. In Sects.6 a brief discussion and conclusions follows.

2 BRIEF REVIEW OF DM

DM is a micromechanical theory based on a discrete material model whereby solids are represented as arrays of points or nodes at finite distances. A pair of such nodes is referred to as a doublet, and the nodal spacing distances introduce length scales into the microstructural theory. Each node in the array is allowed to have a translation and rotation, and increments of these variables are expanded in a Taylor series about the nodal point. The order at which the series is truncated defines the degree of approximation employed. The lowest order case using only a single term in the series will not contain any length scales, while using more than one term will produce a multi length scale theory. This allowable kinematics develops macrostrains of elongation, shear and torsion (about the doublet axis). Through appropriate constitutive assumptions, these micro strains can be related to corresponding elongational, shear and torsional micro stresses. Applications of DM to geo-mechanical problems have been given by Granik and Ferrari [9] and Ferrari et al. [2]. For such applications, a granular interpretation of DM has been employed, in which the material is viewed as an assembly of circular or spherical particles. A pair of such particles represents a doublet as shown in Fig. 1.

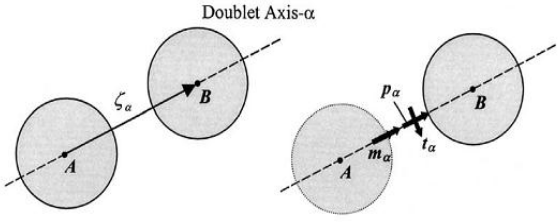

Fig.1
Doublet.

Corresponding to the doublet (*A, B*) there exists a doublet or branch vector $\boldsymbol{\zeta}_a$ connecting the adjacent particle centers and defining the doublet axis. The magnitude of this vector $\eta_a = |\boldsymbol{\zeta}_a|$ is simply the particle diameter for particles in contact. However, in general, the particles need not be in contact, and for this case the length scale η_a could be used to represent a more general microstructural feature. For example, the internal characteristic scale for the crystal lattice parameter of carbon is $\eta_a = 0.1421nm$ [1].

As mentioned, the kinematics allow relative elongational, shearing and torsional motions between the particles, and this is used to develop an elongational micro stress p_a, shear micro stress t_a, and torsional micro stress m_a as shown in Fig. 1. It should be pointed out that these micro stresses are not second order tensors in the usual continuum mechanics sense. Rather, they are vector quantities that represent the elastic micro forces and micro couples of interaction between doublet particles. Their directions are dependent on the doublet axes which are determined by the material microstructure. These micro stresses are not continuously distributed but rather exist only at particular points in the medium being simulated by DM.

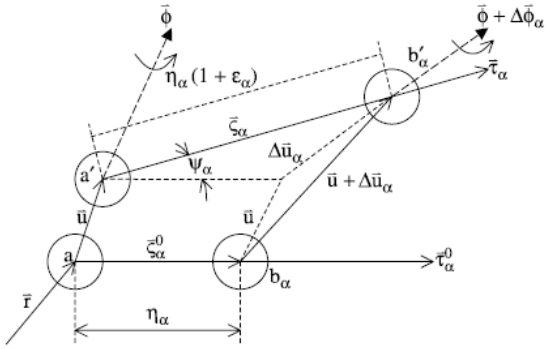

Fig.2
Translations of the doublet nodes $a \in A$, $b_\alpha \in B_\alpha$.

From Fig. 2, suppose doublet (a, b_α) converts to doublet (a', b'_α) because of kinematic translation. The superscript 0 for vectors indicates the initial state.

If $\boldsymbol{u}(\boldsymbol{x},t)$ is the displacement field coinciding with a particle displacement, then the incremental displacement is written as:

$$\Delta\boldsymbol{u}_\alpha = \boldsymbol{u}\left(\boldsymbol{x}+\boldsymbol{\zeta}^0_\alpha, t\right) - \boldsymbol{u}(\boldsymbol{x},t) \tag{1}$$

where $\boldsymbol{x}$ is the position vector of particle.

The incremental function in Eq. (1) could be expanded in a Taylor series as [2]:

$$\Delta\boldsymbol{u}_\alpha = \sum_{\chi=1}^{M} \frac{(\eta_\alpha)^\chi}{\chi!}\left(\boldsymbol{\tau}^0_\alpha.\nabla\right)^\chi \boldsymbol{u} \tag{2}$$

wherein ∇ is the Del operator in general coordinates and η is the internal characteristic length scale. As mentioned above, the number of terms used in the series expansion of the local deformation field determines the order of the approximation in DM.

Here, $\alpha = 1,...,n$ while n is referred to the numbers of doublets. For the problem under study, it is assumed that the shear and torsional micro deformations and micro stresses are negligible and thus only extensional strains and stresses exist.

The extensional micro-strain scalar measure ϵ_α, representing the axial deformation of the doublet vector, is defined as [2]:

$$\epsilon_\alpha = \frac{\boldsymbol{\tau}_\alpha.\Delta\boldsymbol{u}_\alpha}{\eta_\alpha} \tag{3}$$

From Fig. 1, it can be written that

$$\boldsymbol{\tau}_\alpha = \frac{1}{1+\epsilon_\alpha}\left(\boldsymbol{\tau}_\alpha^0 + \frac{\Delta \boldsymbol{u}_\alpha}{\eta_\alpha}\right) \tag{4}$$

As in linear elasticity, it is assumed that the relative displacement $\left|\Delta \boldsymbol{u}_\alpha\right|$ is small compared to the doublet separation distance η_α $(\left|\Delta \boldsymbol{u}_\alpha\right| \ll \eta_\alpha)$ so that it may be assumed that $\boldsymbol{\tau}_\alpha = \boldsymbol{\tau}_\alpha^0$. In nonlinear elasticity $\boldsymbol{\tau}_\alpha \neq \boldsymbol{\tau}_\alpha^0$ and the following approximate relations between $\boldsymbol{\tau}_\alpha$ and $\boldsymbol{\tau}_\alpha^0$ are present [5]

$$\boldsymbol{\tau}_\alpha . \boldsymbol{\tau}_\alpha^0 = \cos(\psi_\alpha) = 1 - \frac{\psi_\alpha^2}{2} \tag{5}$$

$$\boldsymbol{\tau}_\alpha \times \boldsymbol{\tau}_\alpha^0 = \sin(\boldsymbol{\psi}_\alpha) = \boldsymbol{\psi}_\alpha \tag{6}$$

wherein ψ_α is the angle between initial and current branch vectors.

From Eqs. (4)- (6), ψ_α^2 can be obtained as follow

$$\psi_\alpha^2 = \frac{1}{\eta_\alpha^2\left(1+2\epsilon_\alpha+\epsilon_\alpha^2\right)}\left(\Delta \boldsymbol{u}_\alpha \times \boldsymbol{\tau}_\alpha^0\right).\left(\Delta \boldsymbol{u}_\alpha \times \boldsymbol{\tau}_\alpha^0\right) \tag{7}$$

If the two sides of Eq. (4) is multiplied with $\boldsymbol{\tau}_\alpha^0$ and Eqs. (5) and (7) are used, it can be concluded that

$$\frac{1}{\eta_\alpha^2\left(1+2\epsilon_\alpha+\epsilon_\alpha^2\right)}\left(\Delta \boldsymbol{u}_\alpha \times \boldsymbol{\tau}_\alpha^0\right).\left(\Delta \boldsymbol{u}_\alpha \times \boldsymbol{\tau}_\alpha^0\right) = 2 - \frac{2}{1+\epsilon_\alpha}\left(1 + \frac{\Delta \boldsymbol{u}_\alpha . \boldsymbol{\tau}_\alpha^0}{\eta_\alpha}\right) \tag{8}$$

with solving this equation, the micro strain for nonlinear approximation can be obtained. It is clear that for linear approximation that $\Delta \boldsymbol{u}_\alpha \times \boldsymbol{\tau}_\alpha^0 = 0$ and then the linear approximation can be obtained. Multiplication both side of Eq. (8) with $\frac{1}{2}\left(1+2\epsilon_\alpha+\epsilon_\alpha^2\right)$ yields

$$\frac{1}{2\eta_\alpha^2}\left(\Delta \boldsymbol{u}_\alpha \times \boldsymbol{\tau}_\alpha^0\right).\left(\Delta \boldsymbol{u}_\alpha \times \boldsymbol{\tau}_\alpha^0\right) + \left(1+\epsilon_\alpha\right)\left(1 + \frac{\Delta \boldsymbol{u}_\alpha . \boldsymbol{\tau}_\alpha^0}{\eta_\alpha}\right) = 1 + 2\epsilon_\alpha + \epsilon_\alpha^2 \tag{9}$$

In Eq. (9), ignoring ϵ_α^2 in comparison with ϵ_α and $\epsilon_\alpha \frac{\Delta u_{\alpha i}\tau_{\alpha i}^0}{\eta_\alpha}$ in comparison with $\frac{\Delta u_{\alpha i}\tau_{\alpha i}^0}{\eta_\alpha}$, gives the following approximate nonlinear micro strain-displacements equation as:

$$\epsilon_\alpha = \frac{\Delta \boldsymbol{u}_\alpha . \boldsymbol{\tau}_\alpha^0}{\eta_\alpha} + \frac{1}{2\eta_\alpha^2}\left(\Delta \boldsymbol{u}_\alpha \times \boldsymbol{\tau}_\alpha^0\right).\left(\Delta \boldsymbol{u}_\alpha \times \boldsymbol{\tau}_\alpha^0\right) \tag{10}$$

One may write $\boldsymbol{\tau}_\alpha^0 = \tau_{\alpha j}^0 \boldsymbol{e}_j$ where $\tau_{\alpha j}^0$ are the cosines of the angles between the directions of micro stress and the coordinates and $\boldsymbol{e}_i$ is the unit vector in Cartesian coordinate. Setting $\boldsymbol{\tau}_\alpha^0 = \tau_{\alpha i}^0 \boldsymbol{e}_i$, $\Delta \boldsymbol{u}_\alpha = \Delta u_{\alpha i} \boldsymbol{e}_i$ in Eq. (10), it is concluded that

$$\epsilon_\alpha = \frac{1}{2\eta_\alpha^2}\left(\Delta u_{\alpha i}\Delta u_{\alpha i}\tau_{\alpha j}^0\tau_{\alpha j}^0 - \Delta u_{\alpha i}\Delta u_{\alpha j}\tau_{\alpha i}^0\tau_{\alpha j}^0\right)+\frac{\Delta u_{\alpha i}\tau_{\alpha i}^0}{\eta_\alpha} \tag{11}$$

In DM under such assumptions and neglecting temperature effect, the relation between micro strain and micro stress is written in the below [17].

$$p_\alpha = \sum_{\beta=1}^{n} A_{\alpha\beta}\epsilon_\beta \tag{12}$$

wherein p_α is axial micro stress along doublet axes. An example of the axial micro stress is the interatomic forces between atoms or molecules located at the nodes of a general array such as a crystalline lattice. In the case of linear and homogeneous, inter nodal central interactions. Eq. (12) can be interpreted as the constitutive equation in the linear and homogeneous DM and $A_{\alpha\beta}$ is the matrix of the micro modulus of the doublet.

In the homogeneous and isotropic media with local interaction, the above relation is simplified as below [17]:

$$p_\alpha = A_0\epsilon_\alpha \tag{13}$$

The relation between micro stresses and macro stresses is [2, 9]:

$$\boldsymbol{\sigma}^{(M)} = \sum_{\alpha=1}^{n}\boldsymbol{\tau}_\alpha^0\boldsymbol{\tau}_\alpha^0\sum_{\chi=1}^{M}\frac{(-\eta_\alpha)^{\chi-1}}{\chi!}\left(\boldsymbol{\tau}_\alpha^0.\nabla\right)^{\chi-1}p_\alpha \tag{14}$$

Substituting Eq. (11) into Eq. (13) and the result into Eq. (14) and making some manipulations, yields [31]

$$\sigma_{ij} = A_0\sum_{\alpha=1}^{3}\tau_{\alpha i}^0\tau_{\alpha j}^0\tau_{\alpha m}^0\tau_{\alpha n}^0\left(\varepsilon_{mn}+\frac{1}{2\eta_\alpha^2}\tau_{\alpha t}^0\tau_{\alpha s}^0\frac{\partial^2\varepsilon_{mn}}{\partial x_t\partial x_s}\right) \tag{15}$$

This equation is the relation between macro stresses and macrostrain in nonlinear regime. As opposed to the linear algebraic equations between the stress and strains in a local theory, the nonlocal DM theory results in differential relations involving the stresses and the strains. In the following, these relations are presented for homogeneous nanotubes in the isotropic media with local interaction. It is further assumed that all doublets originating from a common node have the same magnitudes, i.e., $\eta_a = \eta, a = 1,2,3$. It is noted that the macromodulii in constitutive Eq. (15) corresponding to the first approximation ($\eta = 0$), is nonscale and indeed independent of chirality means isotropic in the plane (independent to the scale). On the contrary, the macromodulii on the higher approximation ($\eta \neq 0$) are anisotropic. Then, it may be concluded that in the first approximation, Eq. (15) model the continuum-like behavior of solids, whereas in the other approximations, Eq. (15) also reflect discrete-like features of the solid [17]. The three-dimensional equations of motion in DM in the Cartesian coordinate system are given by [26]

$$\frac{\partial\sigma_{ij}^{(M)}}{\partial x_i}+f_i^* = \rho^*\frac{\partial^2 u_j}{\partial t^2} \tag{16}$$

where x_i , $i = 1,2,3$ are the spatial Cartesian coordinates, u_j , $j = 1,2,3$ are the displacement components, t is the time, and ρ^* and f^* are the three dimensional body force and mass density, respectively.

Now, the form of matrix $[\boldsymbol{A}]$ in Eq. (12) containing elastic macro constant for plane problem (two-dimensional) is obtained. For this reason, consider Fig. 3. According to Fig. 3, in the $x_1 - x_2$ plane, there are only three doublets with equal angels between them. The solution for the scale less condition can be calculated directly from the

associated CCM problem for an isotropic material. For the plane problems in the homogeneous media, $[\boldsymbol{A}]$ is a symmetric matrix of order 3 with the most general form [20]

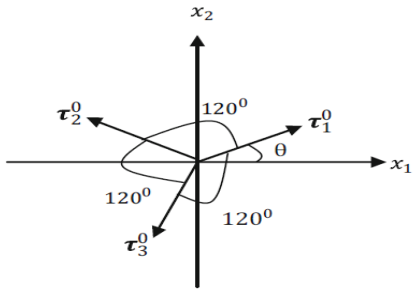

Fig.3
Three doublets with equal angle 120^0 between them.

$$A=\begin{bmatrix} a & b & b \\ b & a & b \\ b & b & a \end{bmatrix} \tag{17}$$

It can be shown that for any θ, if Eq. (17) is substituted into Eq. (12) and plane stress condition is considered, the coefficients a and b in matrix A are found to be [2]:

$$a=\frac{4}{9}\mu\frac{7\lambda+10\mu}{\lambda+2\mu},\ b=\frac{4}{9}\mu\frac{\lambda-2\mu}{\lambda+2\mu} \tag{18}$$

where λ,μ are Lame constants and can be written in term of elasticity modulus E, Poisson ratio v and shear modulus G as below [20]

$$\lambda=\frac{vE}{(1+v)(1-2v)},\ \mu=G=\frac{E}{2(1+v)} \tag{19}$$

One could use $b=0$ as a quantitative guide to the applicability of the simpler constitutive relations such as Eq. (13). If $\lambda=2\mu$ (or $v=\frac{1}{3}$) in plane stress condition from Eq. (18), it is concluded that $b=0$ and

$$a=A_0=\frac{8\mu}{3}=E \tag{20}$$

3 EQUATIONS OF MOTION IN DM

Specific applications of DM have been developed for two-dimensional problems with regular particle packing microstructures. One case that has been studied is the two-dimensional hexagonal packing without internal atoms as shown in Fig. 3. This geometrical microstructure establishes three doublet axes at 120 angles as shown in Fig. 3 is nanostructure. Now, the governing equations for torsional vibration of SWCNTs are derived.

Let the position vector of a point of a shell be denoted by $\boldsymbol{p}\left(\theta^\alpha,\theta^3,t\right),\alpha=1,2$ where θ^α and θ^3 are the contravariant curvilinear components and $\boldsymbol{g}_i$,$i=1,2,3$ be the covariant base vectors of the shell-like body. It may be assumed that $\theta^3=\xi$ where z indicates the thickness direction of the shell. Any point on the surface $\xi=0$ is specified by the position vector $\boldsymbol{r}\left(\theta^\alpha,t\right),\alpha=1,2$. It is evident that $\boldsymbol{r}\left(\theta^\alpha,t\right)=\boldsymbol{p}\left(\theta^\alpha,\theta^3=0,t\right)$. Let

$\boldsymbol{a}_\alpha = \boldsymbol{g}_\alpha\left(\theta^\alpha, \theta^3 = 0, t\right)$ be the surface base vectors, i.e., $\boldsymbol{a}_\alpha\left(\theta^\alpha, t\right) = \boldsymbol{g}_\alpha\left(\theta^\alpha, \theta^3 = 0, t\right)$ and $\boldsymbol{d} = \boldsymbol{g}_3\left(\theta^\alpha, \theta^3 = 0, t\right) = \boldsymbol{a}_3$, then it follows that [39]

$$\boldsymbol{a}_\alpha = \frac{\partial \boldsymbol{r}}{\partial \theta^\alpha}, \alpha = 1,2 \tag{21}$$

with this background in mind, Eq. (16) can be rewritten in curvilinear coordinate as [39]

$$\boldsymbol{T}^{i}_{,i} + \rho^* \boldsymbol{f}^* g^{-\frac{1}{2}} = \rho^* \dot{\boldsymbol{v}}^* g^{-\frac{1}{2}} \tag{22}$$

In Eq. (22) $\mathbf{v}^*$ is the velocity of a point in the shell-like body, which in linear approximation, may be written as [39]

$$\mathbf{v}^*\left(\theta^\alpha, \xi, t\right) = \mathbf{v}\left(\theta^\alpha, t\right) + \xi \boldsymbol{w}\left(\theta^\alpha, t\right) \tag{23}$$

where $\boldsymbol{v}\left(\theta^\alpha, t\right)$ is the velocity of a point on the surface $\xi = 0$ and $\boldsymbol{w} = \dot{\boldsymbol{d}}$ with superposed dot representing the material time derivative. In Eq. (22), g is the determinant of the three dimensional covariant metric tensor g_{ij} and $\boldsymbol{T}^i$ are the surface forces, which may be written as:

$$\boldsymbol{T}^i = g^{\frac{1}{2}}\left(\sigma^{ij}\right)^{(M)} \boldsymbol{g}_j \tag{24}$$

which is related to the surface traction $\boldsymbol{T}$ as [39]

$$\boldsymbol{T} = \boldsymbol{T}^i g^{-\frac{1}{2}} n_i \tag{25}$$

In the above equation $\boldsymbol{n}$ is the outward unit normal to the body. In Eq. (24), $\left(\sigma^{ij}\right)^{(M)}$ are the contravariant components of the macro stress tensor. Let $\boldsymbol{N}$ and $\boldsymbol{M}$ are defined as [39]:

$$\boldsymbol{N}^\alpha a^{\frac{1}{2}} = \int_\alpha^\beta \mathbf{T}^\alpha d\xi, \alpha = 1,2 \tag{26}$$

$$\boldsymbol{M}^\alpha a^{\frac{1}{2}} = \int_\alpha^\beta \xi \mathbf{T}^\alpha d\xi, \alpha = 1,2 \tag{27}$$

where $\boldsymbol{N}^\alpha = N^{\alpha i} a_i$ and $\boldsymbol{M}^\alpha = M^{\alpha i} a_i$. In the above equations, a is the determinant of the two dimensional metric tensor of the surface at $\xi = 0$ and integration is taken along the thickness of the shell wherein α and β are the limits of integration.

Integrating Eqs. (22) with respect to ξ and using physical components of $N^{\alpha i}$ known as the stress resultant, it follows that [39]

$$\frac{1}{a_1 a_2}\left[\left(a_2 N_{11}\right)_{,1} + \left(a_1 N_{21}\right)_{,2} + a_{1,2} N_{12} - a_{2,1} N_{22}\right] + \frac{N_{13}}{r_1} + \rho f_1 = \rho \frac{\partial^2 u_1}{\partial t^2} \tag{28}$$

$$\frac{1}{a_1 a_2}\left[\left(a_2 N_{12}\right)_{,1}+\left(a_1 N_{22}\right)_{,2}-a_{1,2}N_{11}+a_{2,1}N_{21}\right]+\frac{N_{23}}{r_2}+\rho f_2=\rho\frac{\partial^2 u_2}{\partial t^2} \tag{29}$$

$$\frac{1}{a_1 a_2}\left[\left(a_2 N_{13}\right)_{,1}+\left(a_1 N_{23}\right)_{,2}\right]-\left(\frac{N_{11}}{r_1}+\frac{N_{22}}{r_2}\right)+\rho f_3=\rho\frac{\partial^2 u_3}{\partial t^2} \tag{30}$$

wherein r_1 and r_2 are the radii of curvature for the surface, a_1 and a_2 are the magnitudes of the surface base vectors. ρ and f_i are the two dimensional density and two dimensional external body force density, respectively, defined by [32]

$$\rho a^{\frac{1}{2}}=\int_{\alpha}^{\beta}\rho^* g^{\frac{1}{2}} d\xi \tag{31}$$

$$\int_{\beta}^{\beta}\rho^* g^{\frac{1}{2}}\boldsymbol{f}^* d\xi=\rho a^{\frac{1}{2}}\boldsymbol{f}+\left[\boldsymbol{T}^3\right]_{-\frac{h}{2}}^{\frac{h}{2}} \tag{32}$$

Multiplication of both sides of Eq. (22) by ξ and integrating with respect to ξ and using physical components of $M^{\alpha i}$ known as the moment resultant, yields [39]

$$\frac{1}{a_1 a_2}\left[\left(a_2 M_{11}\right)_{,1}+\left(a_1 M_{21}\right)_{,2}+a_{1,2}M_{12}-a_{2,1}M_{22}\right]+\frac{M_{13}}{r_1}+\rho\bar{l}_1=N_{13} \tag{33}$$

$$\frac{1}{a_1 a_2}\left[\left(a_2 M_{12}\right)_{,1}+\left(a_1 M_{22}\right)_{,2}-a_{1,2}M_{11}+a_{2,1}M_{21}\right]+\frac{M_{23}}{r_2}+\rho\bar{l}_2=N_{23} \tag{34}$$

$$\frac{1}{a_1 a_2}\left[\left(a_2 M_{13}\right)_{,1}+\left(a_1 M_{23}\right)_{,2}\right]-\left(\frac{M_{11}}{r_1}+\frac{M_{22}}{r_2}\right)+\rho\bar{l}_3=N_{33} \tag{35}$$

wherein $\bar{\boldsymbol{l}}$ is defined by the following equation [22]

$$\bar{\boldsymbol{l}}=\boldsymbol{l}-k^2\ddot{\boldsymbol{w}} \tag{36}$$

In Eq. (36), $\boldsymbol{l}$ and k^2 respectively, defined by [39]

$$\rho\boldsymbol{l}a^{\frac{1}{2}}=\int_{\alpha}^{\beta}\xi\rho^*\boldsymbol{f}^* g^{\frac{1}{2}} d\xi+\left[\xi\boldsymbol{T}^3\right]_{-\frac{h}{2}}^{\frac{h}{2}} \tag{37}$$

$$k^2=\frac{1}{\rho a^{\frac{1}{2}}}\int_{\alpha}^{\beta}\xi^2\rho^* g^{\frac{1}{2}} d\xi \tag{38}$$

Eqs. (28)- (30) together with Eqs. (33)- (55) are the governing equations for the thin shells in general curvilinear coordinates in DM.

Now consider an SWCNT of length *L*, mean radius *R*, Young's modulus *E*, Poisson's ratio v and mass density ρ as shown in Fig. 4.

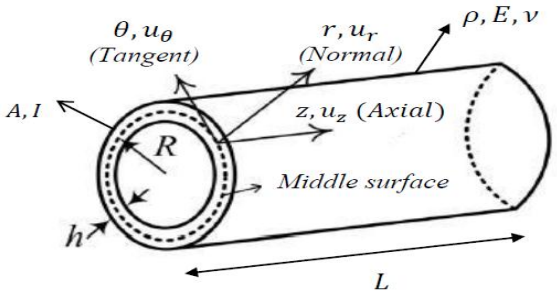

Fig.4
A nanotube in cylindrical coordinate.

In cylindrical coordinate, the coordinate components become [22]

$$\theta_1 = z \ ,\theta_2 = \theta \ ,\theta_3 = r \tag{39}$$

The radii of curvature and the coefficients a_1 and a_2 in cylindrical coordinates are written respectively, as:

$$r_1 = \infty \ ,r_2 = r \tag{40}$$

$$a_1 = \left|\frac{\partial \mathbf{r}}{\partial z}\right| = 1 \ ,a_2 = \left|\frac{\partial \mathbf{r}}{\partial \theta}\right| = r \tag{41}$$

Substituting Eqs. (39)- (41) into Eqs. (28)- (30) and Eqs. (33)- (35), yields

$$\frac{\partial N_{zz}}{\partial z} + \frac{1}{r}\frac{\partial N_{\theta z}}{\partial \theta} + \rho f_z = \rho \frac{\partial^2 u_z}{\partial t^2} \tag{42}$$

$$\frac{\partial N_{z\theta}}{\partial z} + \frac{1}{r}\frac{\partial N_{\theta\theta}}{\partial \theta} + \frac{N_{\theta r}}{r} + \rho f_\theta = \rho \frac{\partial^2 u_\theta}{\partial t^2} \tag{43}$$

$$\frac{\partial N_{zr}}{\partial z} + \frac{1}{r}\frac{\partial N_{\theta r}}{\partial \theta} - \frac{N_{\theta\theta}}{r} + \rho f_r = \rho \frac{\partial^2 u_r}{\partial t^2} \tag{44}$$

$$\frac{\partial M_{zz}}{\partial z} + \frac{1}{r}\frac{\partial M_{\theta z}}{\partial \theta} + \rho \bar{l}_z = N_{zr} \tag{45}$$

$$\frac{\partial M_{z\theta}}{\partial z} + \frac{1}{r}\frac{\partial M_{\theta\theta}}{\partial \theta} + \frac{1}{r}M_{\theta r} + \rho \bar{l}_\theta = N_{\theta r} \tag{46}$$

$$\frac{M_{zr}}{\partial z} + \frac{1}{r}\frac{M_{\theta r}}{\partial \theta} - \frac{M_{\theta\theta}}{r} + \rho \bar{l}_r = N_{rr} \tag{47}$$

which are the equations of motion of a thin shell in the cylindrical coordinates. N_{ij} and M_{ij} in cylindrical coordinates can be obtained by:

$$N_{ij} = \int_{-\frac{h}{2}}^{\frac{h}{2}} \sigma_{ij}^{(M)} dz \ ,i,j = 1,2,3 \tag{48}$$

$$M_{ij} = \int_{-\frac{h}{2}}^{\frac{h}{2}} z\sigma_{ij}^{(M)} dz \ \ ,i,j = 1,2,3 \tag{49}$$

In this study, the following assumptions, known as Love's first approximation, for cylindrical shells are made [25]:

1. All points that lie on a normal to the middle surface before deformation do the same after the deformation. Then the transverse shear stresses $\sigma_{rz}^{(M)}$ and $\sigma_{\theta r}^{(M)}$ are assumed to be negligible.
2. Displacements are small compared to the shell thickness.
3. The normal stresses in the thickness direction ($\sigma_{rr}^{(M)}$) are negligible (planar state of stress).

It should be pointed out that in the radial vibration, all carbon atoms move coherently in the radial direction creating a breathing-like vibration of the entire tube and in the axial vibration, the nanotube vibrates in the longitudinal direction. The coupled radial-axial vibration is the mixing of two vibration modes. Now, Eqs. (42) - (47) are simplified. As the coupled axial-radial vibration in SWCNTs are investigated in this study, then, only Eqs. (42) and (44) which respectively signify axial and radial vibrations are considered. Eq. (43) which is considering torsional vibration is small compared to the axial and radial vibration. Eqs. (45)- (47) are static moment equations which are not used in vibrations. The shear forces may also be neglected because of the first Love's condition then the first and the second terms in Eq. (44) ($\frac{\partial N_{zr}}{\partial z}, \frac{1}{r}\frac{\partial N_{\theta r}}{\partial \theta}$) are removed. On the other hand, in studying the natural frequency, the body forces are ignored then ρf_z and ρf_r are discarded. Furthermore, from the second Love's condition, it is concluded that $\frac{\partial}{\partial r} = 0$ .Assuming axisymmetric condition ($\frac{\partial}{\partial \theta} = 0$), the second term in Eq. (42) ($\frac{1}{r}\frac{\partial N_{\theta z}}{\partial \theta}$) is removed, too.

Assuming homogeneity for the entire tube and that the nanotube vibrates in radial and axial modes only such that the cross-section of the tube is not elastically deformed, it may be concluded that under such assumptions given in the last three paragraphs, Eqs. (42)- (47) are reduced to

$$-\frac{N_{\theta\theta}}{r} = \rho \frac{\partial^2 u_r}{\partial t^2} \tag{50}$$

$$\frac{\partial N_{zz}}{\partial z} = \rho \frac{\partial^2 u_z}{\partial t^2} \tag{51}$$

which are the equation of motion for coupled axial-radial vibration of SWCNTs.

The nonlinear strain-displacement relation is written [5]

$$\boldsymbol{\varepsilon} = \frac{1}{2}\left(\nabla \boldsymbol{u} + \nabla \boldsymbol{u}^T + \nabla \boldsymbol{u}^T \nabla \boldsymbol{u}\right) \tag{52}$$

where ∇ is the gradient operator in cylindrical coordinates given as:

$$\boldsymbol{\nabla} = \frac{\partial}{\partial r}\boldsymbol{e}_r + \frac{1}{r}\frac{\partial}{\partial \theta}\boldsymbol{e}_\theta + \frac{\partial}{\partial z}\boldsymbol{e}_z \tag{53}$$

$\nabla \boldsymbol{u}$ can be written in cylindrical coordinate as [5]

$$\nabla \boldsymbol{u} = \begin{bmatrix} \dfrac{\partial u_r}{\partial r} & \dfrac{1}{r}\left(\dfrac{\partial u_r}{\partial \theta} - u_\theta\right) & \dfrac{\partial u_r}{\partial z} \\ \dfrac{\partial u_\theta}{\partial r} & \dfrac{1}{r}\left(\dfrac{\partial u_\theta}{\partial \theta} + u_r\right) & \dfrac{\partial u_\theta}{\partial z} \\ \dfrac{\partial u_z}{\partial r} & \dfrac{1}{r}\dfrac{\partial u_z}{\partial \theta} & \dfrac{\partial u_z}{\partial z} \end{bmatrix} \tag{54}$$

Substituting Eq. (54) into Eq. (52) and making some manipulations along with considering Eq. (53), yields

$$\varepsilon_{\theta\theta} = \frac{1}{2}\left[2\frac{u_r}{r} + \frac{u_r^2}{r^2}\right] \tag{55}$$

$$\varepsilon_{zz} = \frac{1}{2}\left[2\frac{\partial u_z}{\partial z} + \left(\frac{\partial u_z}{\partial z}\right)^2 + \left(\frac{\partial u_r}{\partial z}\right)^2\right] \tag{56}$$

From Eq. (15), the nonlocal DM constitutive relation for the macroscopic stress takes the following special relations for nanotubes [26, 29]:

$$\sigma_{zz} = E\,\varepsilon_{zz} + \kappa\eta^2 \frac{\partial^2 \varepsilon_{zz}}{\partial z^2} \tag{57}$$

$$\sigma_{\theta\theta} = E\,\varepsilon_{\theta\theta} + \kappa\eta^2 \frac{\partial^2 \varepsilon_{\theta\theta}}{\partial z^2} \tag{58}$$

where E is Young's modulus of the nanotubes. κ is a coefficient depends to chiral of the tube. It is clear that when the nonlocal parameter η is zero, the constitutive relations of the local theories are obtained. If Eqs. (57) and (58) are substituted into Eq. (48), the nonlocal stress resultants are obtained as follow:

$$N_{zz} = Eh\,\varepsilon_{zz} + \kappa h\eta^2 \frac{\partial^2 \varepsilon_{zz}}{\partial z^2} \tag{59}$$

$$N_{\theta\theta} = Eh\,\varepsilon_{\theta\theta} + \kappa h\eta^2 \frac{\partial^2 \varepsilon_{\theta\theta}}{\partial z^2} \tag{60}$$

Now, substituting Eqs. (55) and (56) into Eqs. (59) and (60) and the results into Eqs. (50) and (51) with making some manipulations with neglecting scale effect yields

$$-\frac{E}{1-\nu^2} h\left(u_r + \frac{u_r^2}{2r}\right) = \rho r^2 h \frac{\partial^2 u_r}{\partial t^2} \tag{61}$$

$$Eh\left(\frac{\partial^2 u_z}{\partial z^2} + \frac{\partial u_z}{\partial z}\frac{\partial^2 u_z}{\partial z^2} + \frac{\partial u_r}{\partial z}\frac{\partial^2 u_r}{\partial z^2}\right) = \rho h \frac{\partial^2 u_z}{\partial t^2} \tag{62}$$

Eqs. (61) and (62) are the equations of motion in nonlinear coupled radial-axial vibration of SWCNTs. From these equations, it can be concluded that because of nonlinear terms, the two equations are coupled with together. The fundamental linear equations can be simply calculated by setting the nonlinear terms to zero. In this case, the two equations will be decoupled.

In DM, basic equations of scaling micro dynamics for local interactions with homogeneous medium can be written as follow [2]

$$\rho\ddot{u}_i = \sum_{\kappa=2,4,\ldots}^{R=2M} C_{ijk_1k_2\ldots k_\kappa} \frac{\partial^\kappa u_i}{\partial x_{k_1}\partial x_{k_2}\ldots\partial x_{k_\kappa}} = C_{ijkl}u_{j,kl} + C_{ijklrs}u_{j,klrs} + C_{ijklrspq}u_{j,klrspq} + \ldots \tag{63}$$

where

$$C_{ijk_1k_2\ldots k_\kappa} = 2A_0\sum_{\alpha=1}^{n}\tau_{\alpha i}^0\tau_{\alpha j}^0\tau_{\alpha k_1}^0\tau_{\alpha k_2}^0\ldots\tau_{\alpha k_\kappa}^0\frac{\eta_\alpha^{\kappa-2}}{\kappa!} \tag{64}$$

For coupled axial- radial vibration mode of SWCNTs studied in this paper, Eq. (63) is reduced to Eqs. (61) and Eq. (62). It is noted that the nonscale macro modulus C_{ijkl}, corresponding to $\kappa=2$, is indeed independent of θ, i.e., isotropic in the plane. On the contrary, the macromodulii $C_{ijk_1k_2\ldots k_\kappa}$ for $\kappa=4,6,\ldots$ are anisotropic. Then, it may be concluded that in the first approximation, $\kappa=2$, Eq. (63) model the continuum-like behavior of solids, whereas in the other approximations, $\kappa=4,6,\ldots$ Eq. (63) also reflect discrete-like features of the solid, in a manner that increases with κ [1]. Therefore, it can be concluded that DM theory is capable of modeling solids in view of their dual and to some extent contradictory discrete continuous nature. The power of such dual-representation capability is evident in the discussion of isotropy. The basal plane of the SWCNT is isotropic only in the continuum (nonscale) approximation. Thus, isotropy is a scale-related notion. In fact, no material may be argued to be isotropic at all dimensional scales, down to its most elementary component level [2].

4 APPLICATION OF HPM FOR SOLVING NONLINEAR VIBRATIONS OF SWCNTS

In this section, the nonlinear governing equations for the coupled radial-axial vibration of SWCNTs are solved. The deflection of the nanotube is subjected to the following boundary conditions in radial and axial direction, respectively.

For two clamped (C-C) boundary conditions

$$u_\theta(x,t)=0, u_z(x,t)=0 \ at\ x=0,L \tag{65}$$

For two free (F-F) boundary conditions

$$\frac{\partial u_\theta(x,t)}{\partial x}=0, \frac{\partial u_z(x,t)}{\partial x}=0 at\ x=0,L \tag{66}$$

For clamped-free (C-F) boundary condition

$$u_\theta(x,t)=0, u_z(x,t)=0 at\ x=0, \frac{\partial u_\theta(x,t)}{\partial x}=0, \frac{\partial u_z(x,t)}{\partial x}=0 at\ x=L \tag{67}$$

Now, the nonlinear equations of motion are solved to obtain the nonlinear natural frequencies. Assuming $u_\theta(x,t)=\varphi(x)U(t)$ and $u_z(x,t)=\psi(x)W(t)$ where $\varphi(x)$ and $\psi(x)$ are the Eigen modes of the tube satisfying the kinematic boundary conditions and $U(t)$ and $W(t)$ are the time-dependent deflection parameters of the nanotube. The base functions corresponding to the above boundary conditions are given in Table 1.

Table 1
Common boundary conditions for the axial direction.

End conditions of beam	Mode shape (normal function)
Two clamped (C-C)	$sin\left(\frac{n\pi}{L}x\right)$
Two free (F-F)	$cos\left(\frac{n\pi}{L}x\right)$
Clamped-free (C-F)	$1-cos\left(\frac{2n\pi}{L}x\right)$

Applying the Galerkin method, the governing equations of motion are obtained as follows:

$$-\frac{E}{1-\nu^2}\left[a_1U+\frac{1}{2r}a_2U^2\right]=\rho r^2 a_1\frac{\partial^2 U}{\partial t^2} \tag{68}$$

$$E\left[a_3W+a_4W^2+a_5U^2\right]=\rho a_6\frac{\partial^2 W}{\partial t^2} \tag{69}$$

The above equations are the differential equations of motion governing the nonlinear coupled axial-radial vibrations of SWCNTs subjected to the following initial conditions:

$$U(0)=0,\frac{dU}{dt}(0)=U_{max} \tag{70}$$

$$W(0)=0,\frac{dW}{dt}(0)=W_{max} \tag{71}$$

wherein U_{max} and W_{max} denote the maximum velocities of oscillation in circumferential and radial directions, respectively. In Eqs. (68) and (69), $\alpha_1,\alpha_2,...,\alpha_6$ are as follows:

$$\alpha_1=\int_0^L\varphi^2(z)dz,\alpha_2=\int_0^L\varphi^3(z)dz \tag{72}$$

$$\alpha_6=\int_0^L\psi^2(z)dz,\alpha_4=\int_0^L\psi''(z)\psi'(z)\psi(z)dz,\alpha_5=\int_0^L\varphi''(z)\varphi'(z)\psi(z)\psi(z)dz,\alpha_3=\int_0^L\psi''(z)\psi(z)dz \tag{73}$$

Changing the variable $\tau=\omega t,\nu=\Omega t,a=\frac{U}{r},b=\frac{W}{r}$ and $r=\sqrt{\frac{I}{A}}$, Eqs. (68) and (69) can be transformed to the following nonlinear equation:

$$\omega^2\frac{d^2a}{\partial\tau^2}+Aa+Ba^2=0 \tag{74}$$

$$\Omega^2\frac{d^2b}{\partial\nu^2}+Cb+Db^2+Ea^2=0 \tag{75}$$

wherein ω and Ω are respectively the nonlinear axial and radial frequencies in the coupled nonlinear axial-radial vibration of SWCNTs. The coefficients A,B,C,D and E are defined by the following equations

$$A = \frac{E}{\rho r^2 \left(1-\nu^2\right)} = \omega_L^2 \tag{76}$$

$$B = \frac{E}{2\rho r^3 \left(1-\nu^2\right)} \frac{\alpha_2}{\alpha_1} \sqrt{\frac{I}{A}} \tag{77}$$

$$C = -\frac{E}{\rho} \frac{\alpha_3}{\alpha_6} = \Omega_L^2 \tag{78}$$

$$D = -\frac{1}{2} \frac{\alpha_4}{\alpha_6} \sqrt{\frac{I}{A}} \frac{E}{\rho} \tag{79}$$

$$E = -\frac{1}{2} \frac{\alpha_5}{\alpha_6} \sqrt{\frac{I}{A}} \frac{E}{\rho} \tag{80}$$

In Eqs. (76) and (78), $\omega_L = \sqrt{A}$ and $\Omega_L = \sqrt{C}$ is the linear, free vibration frequency in the radial and axial vibration modes, respectively and the unknown angular frequency has to be determined. To this end, New HPMs are applied to seek the solution of Eqs. (74) and (75). The following homotopies with ω_0 and Ω_0 as the initial approximations for the angular frequency are considered

$$\left(1-p\right)\omega_0^2 \left(\frac{d^2 a}{\partial \tau^2} + a\right) + p\left(\omega^2 \frac{d^2 a}{\partial \tau^2} + Aa + Ba^2\right) = 0 \tag{81}$$

$$\left(1-p\right)\Omega_0^2 \left(\frac{d^2 b}{\partial \nu^2} + b\right) + p\left(\Omega^2 \frac{d^2 b}{\partial \nu^2} + Cb + Db^2 + Ea^2\right) = 0 \tag{82}$$

Here p is a parameter, $a = a\left(\tau, p\right)$, $b = b\left(\nu, p\right)$, $\omega = \omega\left(p\right)$ and $\Omega = \Omega\left(p\right)$. Obviously, when $p = 0$, Eqs. (81) and (82) yields the following linear harmonic equations

$$\frac{d^2 a}{\partial \tau^2} + Aa = 0 \ , a\left(0\right) = 0 \ , \frac{da\left(0\right)}{\partial \tau} = X \tag{83}$$

$$\frac{d^2 b}{\partial \nu^2} + Cb = 0 \ , b\left(0\right) = 0 \ , \frac{db\left(0\right)}{\partial \nu} = Y \tag{84}$$

It is notable that for $p = 1$, it results the nonlinear Eqs. (74) and (75), respectively. As, parameter p varies from 0 to 1, the solutions $a = a\left(\tau, p\right)$ and $\omega = \omega\left(p\right)$ along with $b = b\left(\nu, p\right)$, $\Omega = \Omega\left(p\right)$ of the homotopy Eqs. (81) and (82) change from their initial approximations $a_0\left(\tau\right), \omega_0$ and $b_0\left(\nu\right), \Omega_0$ to the required solutions $a\left(\tau\right), \omega$ and $b\left(\nu\right), \Omega$ of Eqs. (74) and (75), respectively. Suppose the solution of Eqs. (81) and (82) to be in the following forms:

$$a\left(\tau\right) = a_0\left(\tau\right) + p a_1\left(\tau\right) + \ldots \tag{85}$$

$$\omega = \omega_0 + p\omega_1 + \ldots \tag{86}$$

$$b(\nu)=b_0(\nu)+pb_1(\nu)+\ldots \tag{87}$$

$$\Omega=\Omega_0+p\Omega_1+\ldots \tag{88}$$

Substituting the above relations into the Eqs. (81) and (82), respectively and equaling the coefficients of the terms with same powers of p, the following linear differential equations are obtained

$$\begin{aligned} &p^0:\frac{d^2a_0}{\partial\tau^2}+Aa_0=0,a_0(0)=0,\frac{da_0(0)}{\partial\tau}=X\\ &p^1:\omega_0^2\left(\frac{d^2a_1}{\partial\tau^2}+Aa_1\right)+\left(\omega^2\frac{d^2a_0}{\partial\tau^2}+Aa_0+Ba_0^2\right)=0,a_1(0)=0,\frac{da_1(0)}{\partial\tau}=0 \end{aligned} \tag{89}$$

$$\begin{aligned} &p^0:\frac{d^2b_0}{\partial\nu^2}+Ab_0=0,b_0(0)=0,\frac{db_0(0)}{\partial\nu}=Y\\ &p^1:\Omega_0^2\left(\frac{d^2b_1}{\partial\nu^2}+Ab_1\right)+\left(\Omega^2\frac{d^2b_0}{\partial\nu^2}+Cb_0^2+Ea_0^2\right)=0,b_1(0)=0,\frac{db_1(0)}{\partial\nu}=0 \end{aligned} \tag{90}$$

The solution of the initial zero approximation is simply given by

$$a_0(\tau)=X\sin(\tau) \tag{91}$$

$$b_0(\nu)=Y\sin(\nu) \tag{92}$$

Substituting Eqs. (91) and (92) into the first approximations of Eqs. (89) and (90), respectively, it is obtained

$$\omega_0^2\left(\frac{d^2a_1}{\partial\tau^2}+a_1\right)+\left[-\omega_0^2X\sin(\tau)+AX\sin(\tau)+BX^2\sin^2(\tau)\right]=0 \tag{93}$$

$$\Omega_0^2\left(\frac{d^2b_1}{\partial\nu^2}+b_1\right)+\left[-\Omega_0^2Y\sin(\nu)+CY\sin(\nu)+DY^2\sin^2(\nu)+EX^2\sin^2(\nu)\right]=0 \tag{94}$$

Expanding the trigonometric function using Fourier sine series for $\sin^2(\tau)$ in the first period yields

$$\sin^2(\tau)\cong\frac{8}{3\pi}\sin(\tau)-\frac{8}{15\pi}\sin(3\tau) \tag{95}$$

Substituting Eq. (95) into Eqs. (93) and (94) and letting the coefficient of $\sin(\tau)$ to be zero in order to eliminate the secular terms, it is found that

$$\omega=\sqrt{A+\frac{8}{3\pi}BX} \tag{96}$$

$$\Omega=\sqrt{C+\frac{8}{3\pi}\left(DY+E\frac{X^2}{Y}\right)} \tag{97}$$

It can also be seen that in contrast to linear systems, the frequencies of the vibration are dependent on its velocity amplitude which are related to the initial conditions so that the larger the amplitude, the more pronounced the discrepancy between the linear and nonlinear frequencies becomes. This is caused by the nonlinearity of the system. It should be noted that if the dependence of the frequencies to amplitudes of vibration is neglected, the linear natural frequencies of the system are obtained. The results demonstrate that the nonlinear axial natural frequency is deviated from the linear part only by the axial vibration amplitude while the nonlinear radial natural frequency is dependent on the axial and radial vibration velocities of the system.

Considering Eqs. (96) and (97), the solution of Eqs. (93) and (94) can be obtained as:

$$a_1(\tau)=\frac{3}{5}\frac{BX^2}{3\pi A+8BX}\left[\sin(\tau)-\frac{1}{3}\sin(3\tau)\right] \tag{98}$$

$$b_1(\nu)=\frac{3}{5}\frac{EY^2+DX^2}{3\pi YC+8\left(EY^2+DX^2\right)}\left[\sin(\nu)-\frac{1}{3}\sin(3\nu)\right] \tag{99}$$

Thus, the first approximate solution of Eqs. (74) and (75) can be written as follows:

$$a(\tau)=a_0(\tau)+a_1(\tau)=X\sin(\tau)+\frac{3}{5}\frac{BX^2}{3\pi A+8BX}\left[\sin(\tau)-\frac{1}{3}\sin(3\tau)\right] \tag{100}$$

$$b(\nu)=b_0(\nu)+b_1(\nu)=Y\sin(\nu)+\frac{3}{5}\frac{DY^2+EX^2}{3\pi YC+8\left(DY^2+EX^2\right)}\left[\sin(\nu)-\frac{1}{3}\sin(3\nu)\right] \tag{101}$$

5 RESULTS AND DISCUSSION

To validate the present method for the analysis of the coupled radial- axial vibration of the tube, first the developed model is validated by comparing the simulated results with those available in literature. In Fig. 5, the relations of radial and axial frequencies of an Armchair (10, 10) SWCNT with radius R=0.678 nm and wall thickness $2h$=0.09 nm are presented for the axisymmetric condition. Comparisons are made with the corresponding results obtained from [38] using the wavelet based spectral element method. In this figure, the frequencies in optical units are presented for varying longitudinal wavenumber K_z normalized as $K_z a$ wherein $a=R-\frac{h}{2}$. The bulk material properties are, Young's modulus $Eh=360\frac{J}{m^2}$ mass density $\rho h=2270\frac{kg}{m^3}$, and Poisson's ratio $v=0.2$ as the same as [38]. The frequencies are expressed in optical units cm^{-1}, where the conversion is given as $1Hz=3.336\times10^{-11}cm^{-1}$.

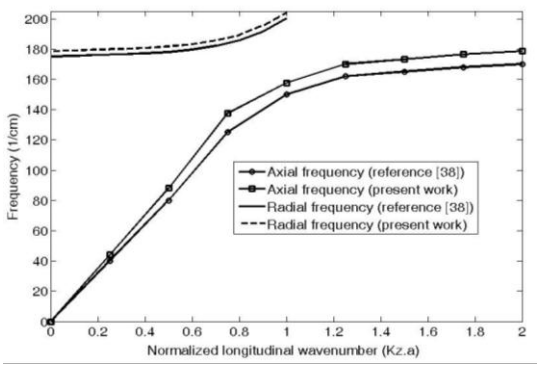

Fig.5
Axial and radial frequencies versus normalized longitudinal wavenumber.

From the above figure, it can be seen that the radial and axial frequencies predicted by the present model is in good agreement with that obtained from [38].

Another comparison between the results obtained herein using HPM method and the available numerical results are presented. To this end, the variation of nondimensional vibration amplitude for axial modes is plotted versus the nondimensional time for Zigzag (16, 0) SWCNT using fourth-order Runge-Kutta method and presented method in Fig. 6. From this figure, it can be seen that the HPM predictions of the nonlinear axial frequency are in good agreement with the forth-ordered Runge-Kuta numerical results. The boundary condition is assumed to be clamped-free. The material properties of SWCNT are taken to be: Young's modulus $E = 1.1\ TPa$, mass density $\rho = 2300 \frac{kg}{m^3}$ and Poisson's ratio $v = 0.2$ [1].

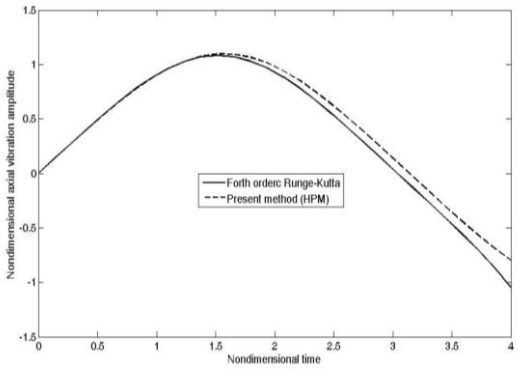

Fig.6
Nondimensional axial vibration amplitude versus nondimensional time for Zigzag (16, 0) nanotube with $X=Y=1$ for clamped-free boundary condition.

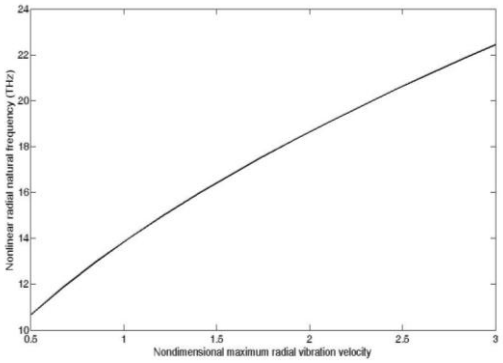

Fig.7
Nonlinear radial natural frequency against nondimensional maximum radial vibration velocity for Zigzag (16, 0) SWCNTs with clamped-free boundary condition.

Figs. 7 and 8 show the nonlinear natural frequencies variation versus maximum radial and axial vibration velocities for Zigzag (16, 0), respectively. As can be seen from these figures, in contrast to linear systems, the nonlinear natural frequencies are a function of maximum vibration velocity so that the larger the velocity, the more pronounced the discrepancy between the linear and nonlinear frequencies become. It should be noted that in the case $B = 0$ in Eq. (96) and also $D = E = 0$ in Eq. (97), the results are in a complete agreement with those obtained via linear method according to the formulations presented in [26, 29].

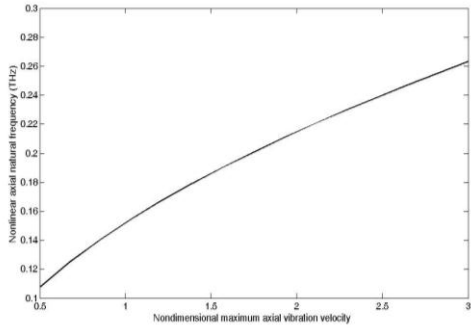

Fig.8
Nonlinear axial natural frequency against nondimensional maximum axial vibration velocity for Zigzag (16, 0) SWCNTs with clamped-free boundary condition.

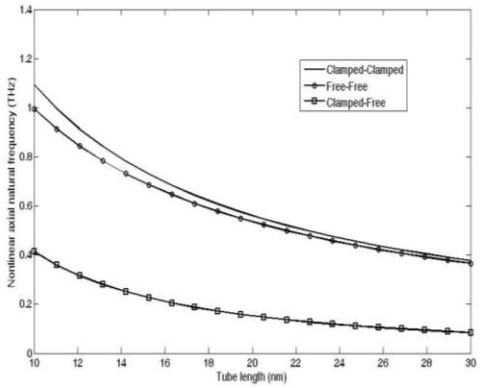

Fig.9
Variation of nonlinear axial natural frequencies against tube length for Zigzag (16, 0) SWCNT with Y=1 under various boundary conditions.

Fig. 9 illustrates the nonlinear axial natural frequency variation against to the tube length for Zigzag (16, 0) SWCNT under different boundary conditions. It can be observed that with the increase of the tube length, the nonlinear natural frequencies of SWCNTs decrease. This decreasing is more apparent for lower lengths. As is expected, the clamped CNT has the highest natural frequency among the selected boundary conditions. It is also seen that as the tube length increases, the nonlinear frequencies tend to approach the linear ones especially for large lengths.

Variation of nonlinear natural axial frequency versus tube diameter has been plotted in Fig. 10 for different vibration modes. As seen from this figure, as the tube diameter increases the nonlinear axial natural frequency increases, too. This increasing is more apparent in higher modes of vibration and higher tube diameter. It is also seen that as the vibration mode increases, the nonlinear natural frequency increases too.

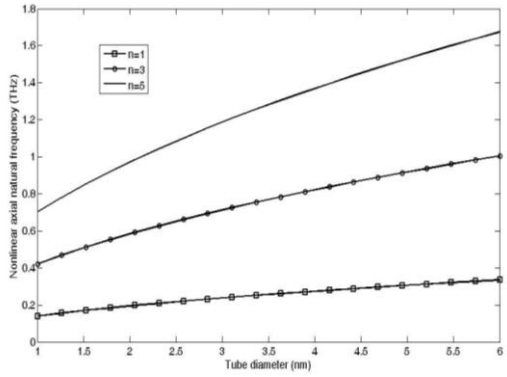

Fig.10
Variation of nonlinear axial natural frequency versus tube diameter with Y=1 for various modes of vibration.

6 CONCLUSIONS

In this paper, a detailed investigation of the nonlinear coupled axial-radial vibration of SWCNTs based on HPM has been presented. The equations of motion for nonlinear coupled axial-radial vibration of the SWCNT are derived based on nonlocal theory. It is the first time that nonlocal theory has been used to analyze the nonlinear coupled axial-radial vibration of SWCNTs. The nonlinearities were originated from the large deformations in interaction of radial and axial modes. To obtain the nonlinear frequency equations in coupled axial-radial mode, the HPM has been used to derive the nonlinear natural frequencies of SWCNTs with arbitrary end conditions. It is notable that HPM is straightforward and powerful, and it is a promising technique for solving strong nonlinear partial differential equations like nonlinear coupled axial-radial vibration of SWCNTs. The significant dependency of these nonlinear natural frequencies to tube radius, tube length and the maximum vibration velocity are studied in different boundary conditions and mode numbers. To show the accuracy and ability of this method, the generated results obtained have been compared with numerical and excellent correlation has been achieved. The main results specifically obtained in this paper are as follows.

1- Due to the coupling of the axial and radial vibrations and obtaining the nonlinear natural frequencies in radial and axial modes of vibrations, radial and axial nonlinear natural frequencies are defined in this

analysis. The nondependent part of the nonlinear natural frequencies to the velocity of vibration represents the natural frequencies of the linear model in which the radial and axial vibrations are decoupled with together.

2- The nonlinear natural frequencies of the system are obtained as the functions of maximum axial and radial vibration velocities which this phenomenon is due to nonlinear nature of the system.
3- The coupling between the radial and axial vibrations appears in the nonlinear higher order free vibrations of the SWCNT which is originated from the large deformation terms in the deriving of the nonlinear differential equations of the system. This interaction generally affects the global dynamic behavior of the SWCNT.
4- The nonlinearity leads to increment of the natural frequencies comparing with the linear model such that the nonlinear natural frequencies are higher than its linear counterparts.
5- As one travels through the end conditions of C-F, to fully clamped, denoted by C-C, respectively, the influence of the boundary conditions is shown to increase the natural frequencies. This effect is more significant for lower values of tube length.
6- The nonlinear natural frequencies increase by the increase in the value of the tube diameter. This effect is more observed in higher mode numbers. It means that the effect of nonlinearity is intensified at the higher modes of vibration.
7- As the tube length increase, the natural frequencies decrease. This decreasing is more apparent in clamped boundary condition and higher vibration mode. This shows that the effect of interaction of the radial and axial vibrations of the SWCNTs decreases with increase in tube length. But an inverse effect is observed in increasing the tube diameter.

ACKNOWLEDGEMENTS

Authors are thankful to “Shahryar Branch, Islamic Azad University, Shahryar, Iran” for providing research facilities. This paper is the product of a research project entitled “Derivation of equation of motion for nonlinear vibration of nanotubes using doublet mechanics theory and solving it via numerical methods” which has been approved and supported by Shahryar Branch, Islamic Azad University, Shahryar, Iran.

REFERENCES

[1] Fatahi-Vajari A., 2018, A new method for evaluating the natural frequency in radial breathing like mode vibration of double-walled carbon nanotubes, *ZAMM* **98**(2): 255-269.
[2] Ferrari M., Granik V.T., Imam A., Nadeau J., 1997, *Advances in Doublet Mechanics*, Springer, Berlin.
[3] Bachilo S.M., Strano M.S., Kittrell C., Hauge R.H., Smalley R.E., Weisman R.B., 2002, Structure-assigned optical spectra of single-walled carbon nanotubes, *Science* **298**: 2361-2366.
[4] Rao A., Richter E., Bandow S., Chase B., Eklund P., Williams K., Fang S., Subbaswamy K., Menon M., Thess A., 1997, Diameter-selective Raman scattering from vibrational modes in carbon nanotubes, *Science* **275**(5297): 187-191.
[5] Fatahi-Vajari A., Azimzadeh Z., 2018, Analysis of nonlinear axial vibration of single-walled carbon nanotubes using Homotopy perturbation method, *Indian Journal of Physics* **92**(11): 1425-1438.
[6] Sanchez-Portal D., Artacho E., Soler J.M., Rubio A., Ordejon P., 1999, Ab initio structural, elastic, and vibrational properties of carbon nanotubes, *Physical Review B* **59**(19): 12678.
[7] Gupta S.S., Batra R.C., 2008, Continuum structures equivalent in normal mode vibrations to single-walled carbon nanotubes, *Computational Materials Science* **43**: 715-723.
[8] Gupta S.S., Bosco F.G., Batra R.C., 2010, Wall thickness and elastic moduli of single-walled carbon nanotubes from frequencies of torsional, torsional and in extensional modes of vibration, *Computational Materials Science* **47**: 1049-1059.
[9] Granik V.T., Ferrari M., 1993, Microstructural mechanics of granular media, *Mechanics of Materials* **15**: 301-322.
[10] Iijima S., 1991, Helical microtubes of graphitic carbon, *Nature* **354**: 56-58.
[11] Pal H., Sharma V., 2015, Effect of sintering on mechanical and electrical properties of carbon nanotube based silver nanocomposites, *Indian Journal of Physics* **89**(3): 217-224.
[12] Ghosh P., Soga T., Afre R.A., Jimbo T., 2008, Simplified synthesis of single-walled carbon nanotubes from a botanical hydrocarbon, Turpentine oil, *Journal of Alloys and Compounds* **462**: 289-293.
[13] Bachilo S.M., Strano M.S., Kittrell C., Hauge R.H., Smalley R.E., Weisman R.B., 2002, Structure-assigned optical spectra of single-walled carbon nanotubes, *Science* **298**: 2361-2366.
[14] Sadd M.H., 2005, *Elasticity Theory, Applications, and Numeric*, Elsevier Butterworth-Heinemann, Burlington.

[15] Mirtalaie S.H., Hajabasi M.A., 2017, Nonlinear axial-lateral-torsional free vibrations analysis of Rayleigh rotating shaft, *Archive of Applied Mechanics* **87**(9): 1465-1494.
[16] Ishida Y., Yamamoto T., 2012, *Linear and Nonlinear Rotordynamics*, Wiley-VCH, Weinheim.
[17] Fatahi-Vajari A., Imam A., 2016, Lateral vibration of single-layered graphine sheets using doublet mechanics, *Journal of Solid Mechanics* **8**(4): 875-894.
[18] Ansari R., Gholami R., Rouhi H., 2012, Vibration analysis of single-walled carbon nanotubes using different gradient elasticity theories, *Composites: Part B* **43**: 2985-2989.
[19] Elishakoff I., Pentaras D., 2009, Fundamental natural frequencies of double-walled carbon nanotubes, *Journal of Sound and Vibration* **322**: 652-664.
[20] Fatahi-Vajari A., Azimzadeh, Z., 2020, Natural frequency of rotating single-walled carbon nanotubes with considering gyroscopic effect, *Journal of Solid Mechanics* **12**(1):136-147.
[21] Bocko J., Lengvarský P., 2014, Bending vibrations of carbon nanotubes by using nonlocal theory, *Procedia Engineering* **96**: 21-27.
[22] Fatahi-Vajari A., Imam A., 2016, Torsional vibration of single-walled carbon nanotubes using doublet mechanics, *ZAMP* **67**: 81.
[23] Gheshlaghi B., Hasheminejad S.M., Abbasion S., 2010, Size dependent torsional vibration of nanotubes, *Physica E* **43**: 45-48.
[24] Arda M., Aydogdu M., 2015, Analysis of free torsional vibration in carbon nanotubes embedded in a viscoelastic medium, *Advances in Science and Technology Research Journal* **9**(26): 28-33.
[25] Selim M.M., 2009, Torsional vibration of carbon nanotubes under initial compression stress, *Brazilan Journal of* Physics **40**(3): 283-287.
[26] Fatahi-Vajari A., Imam A., 2016, Analysis of radial breathing mode of vibration of single-walled carbon nanotubes via doublet mechanics, *ZAMM* **96**(9): 1020-1032.
[27] Liand Q.M., Shi M. X., 2008, Intermittent transformation between radial breathing and flexural vibration modes in a single-walled carbon nanotube, *Proceeding of the Royal Society A* **464**: 1941-1953.
[28] Demir C., Civalek O., 2013, Torsional and longitudinal frequency and wave response of microtubules based on the nonlocal continuum and nonlocal discrete models, *Applied Mathematical Modeling* **37**: 9355-9367.
[29] Fatahi-Vajari A., Imam A., 2016, Axial vibration of single-walled carbon nanotubes using doublet mechanics, *Indian Journal of Physics* **90**(4): 447-455.
[30] Aydogdu M., 2012, Axial vibration analysis of nanorods (carbon nanotubes) embedded in an elastic medium using nonlocal elasticity, *Mechanics Research Communications* **43**: 34-40.
[31] Fatahi-Vajari A., Azimzadeh Z., 2019, Axial vibration of single-walled carbon nanotubes with fractional damping using doublet mechanics*, Indian Journal of Physics* **94**: 975-986.
[32] He J.H., 1998, Approximate analytical solution for seepage flow with fractional derivatives in porous media, *Computer Methods in Applied Mechanics and Engineering* **167**: 57-68.
[33] He J.H., 2006, Homotopy perturbation method for solving boundary value problems, *Physics Letters, Section A* **350**(1-2): 87-88.
[34] Vahidi A.R, Azimzadeh Z., Didgar M., 2013, An efficient method for solving Riccati equation using homotopy perturbation method*, Indian Journal of Physics* **87**(5): 447-454.
[35] Cveticanin L., 2009, Application of homotopy-perturbation to nonlinear partial differential equations, *Chaos, Solitons & Fractals* **40**(1): 221-228.
[36] Azimzadeh Z., Vahidi A.R., Babolian E., 2012, Exact solutions for non-linear Duffing's equations by He's homotopy perturbation method, *Indian Journal of Physics* **86**(8): 721-726.
[37] Azimzadeh Z., Fatahi-Vajari A., 2019, Coupled axial-radial vibration of single-walled carbon nanotubes via doublet mechanics, *Journal of Solid Mechanics* **11**(2): 323-340.
[38] Mitra M., Gopalakrishnan S., 2007, Vibrational characteristics of single-walled carbon-nanotube: Time and frequency domain analysis, *Journal of Applied Physics* **101**: 114320.1-114320.9.
[39] Green A.E., Zerna W., 1968, *Theoretical Elasticity*, Dover Publication, INC, New York.
[40] Naghdi P.M, 1972, *The Theory of Shells and Plates*, In S. Flugge's Handbuch der Physik, Springer- Verlag.